

Persistent Droplet Motion in Liquid-Liquid Dewetting

Matti Oron,^{1,*} Tobias Kerle,^{1,†} Rachel Yerushalmi-Rozen,^{2,‡} and Jacob Klein^{1,3,§}

¹Materials and Interfaces Department, Weizmann Institute of Science, Rehovot 76100, Israel

²Chemical Engineering Department, Ben Gurion University, Beer Sheva 84105, Israel

³Physical and Theoretical Chemistry Laboratory, Oxford University, Oxford OX1 3QZ, United Kingdom

(Received 11 January 2004; published 11 June 2004)

When a nonvolatile liquid film dewets from a partly compatible liquid substrate, the advancing dewetting front leaves behind droplets formed through a Rayleigh instability mechanism at its rim. We have found that these droplets continue to move in the direction of the dewetting front for extended periods (of order one day) with an initial droplet velocity varying linearly with the droplet size, and a displacement varying logarithmically with time. We attribute this persistent motion to a transient surface tension gradient on the substrate liquid surface trailing the dewetting front.

DOI: 10.1103/PhysRevLett.92.236104

PACS numbers: 68.05.-n, 47.20.Dr

The spontaneous breakup and contraction of liquid films from substrates that they do not fully wet—dewetting—is an everyday phenomenon with considerable practical importance, and has been studied and analyzed since at least the time of Laplace [1–3]. The dewetting of a nonvolatile liquid film (say, *A*) from a planar solid substrate (*B*) is reasonably well understood; as the rim of *A* recedes from a dewetted region, it breaks up by Rayleigh instability leaving stationary droplets behind on the surface of *B*. Recently we reported on the dewetting of a liquid film from a liquid substrate with which it is partly compatible (each of the coexisting phases containing some 10% of the minority component), initiated by a Marangoni-like effect at the sample edges [4,5]. For such liquid-liquid dewetting, droplets of *A* are also shed at the receding *A* front [e.g., inset of Fig. 1(b)], but, in contrast to liquid-solid dewetting, such droplets persist in their motion for extended periods. This droplet motion appears intrinsic to liquid-liquid dewetting, contrasting with situations where droplets driven by gradients, either of surface temperature or of surfactant-induced surface tension, have been seen to move freely on solid surfaces [6–9]. Here we investigate the origin of this motion, and show that this remarkably persistent effect is consistent with a weak, slowly relaxing lateral composition gradient at the dewetted liquid substrate, arising from the fact that the two liquid phases are partly compatible.

The liquids used were hydrogenated oligomeric styrene (hOS, Polymer Laboratories, U.K.), deuterated oligomeric styrene (dOS), and oligomeric ethylene-propylene (OEP). Their characteristics are given in Table I. The hOS and dOS are both only slightly miscible with the OEP, and all are Newtonian liquids. Bilayers of the OEP and either the hOS or dOS were created by spin casting a symmetric mixture of the two from a common solvent (toluene) onto gold-coated silicon wafers, forming a thin film that rapidly phase separated into two coexisting planar liquid layers. Each layer is ca. 90% enriched in the majority component (either hOS, dOS, or OEP), with an interfacial

region of ca. 30 nm width between the layers [5]. Droplets shed by the dewetting front [inset of Fig. 1(b)] as it moves from the edges inwards towards the sample center persist in their motion for extended periods. This is seen in Figs. 1(a) and 1(b) (for the couple dOS/OEP), which

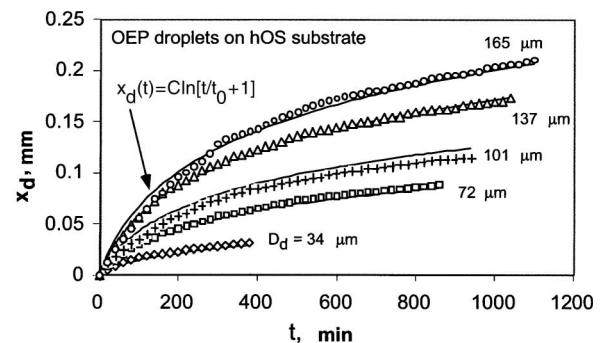
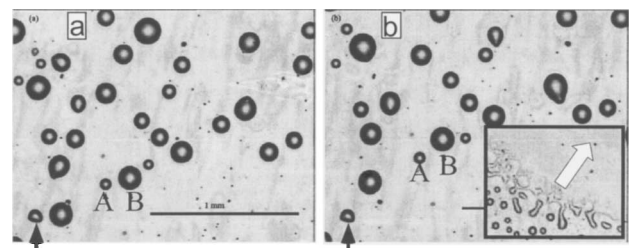


FIG. 1. dOS-rich droplets on an OEP-rich substrate following dewetting by the overlying dOS-rich film. (b) is imaged 70 min following (a), and shows the displacement of droplets relative to an impurity-pinned (stationary) droplet (arrows). *A* and *B* are two droplets of different cap diameter, showing clearly that the larger droplets move faster. The inset of (b) shows the motion of the front as it sheds droplets at its rim. (c) Position x_d of OEP droplets on an hOS substrate as a function of time t after being shed from the dewetting OEP film. Droplet cap diameters D_d are indicated. The solid curves correspond to Eq. (3) (indicated), with the single value $C/D_d = 0.44$ and $t_0 = 62.5$ min used for all curves. Where the solid curves cannot be distinguished they are overlaid by the data points.

TABLE I. Characteristics of liquids used.

Liquid	M_w (g/mole)	η (298 K) (Poise)	T_g (K)	γ (mN/m)
hOS	580	~ 100	255	30–32
dOS	580	15	250	29–32
OEP	2000	50	213	30–33

also show that larger droplets move faster. Figure 1(c) summarizes the motion for 5 droplets of differing cap sizes in a different dewetting experiment (using the couple OEP/hOS).

What causes such persistent droplet motion? It is clearly not an inertial effect; rather, it must be driven by a gradient ($\partial\gamma/\partial x$) in surface tension γ , where x is the direction of motion of the dewetting front, which the droplets follow. The origin of this gradient may be attributed with the help of Fig. 2. Far from the dewetting rim, on the right-hand side (RHS) of Fig. 2 (cut *a*), the two liquid layers are in coexistence, with the composition profile between them—directly determined via nuclear reaction analysis [5]—as indicated in the lower RH composition (ϕ_A) depth (z) profile. At the interface midplane at S , the compositions $\phi_A \equiv \phi_{A,S} \approx \phi_B \equiv \phi_{B,S} \approx 0.5$ are roughly equal. When the top (*A*-rich) liquid layer dewets, its front detaches at position x_1 (say, at time t_1) from the (*B*-rich) lower liquid substrate. The interfacial composition or volume fractions $\phi_{A,S}, \phi_{B,S}$ at x_1 must then instantaneously correspond to their value at the midplane S of the interfacial region between the coexisting *A*-enriched and the *B*-enriched layers, i.e., $\phi_{A,S} \approx \phi_{B,S} \approx 0.5$. This is indicated in cut *b* (Fig. 2) and the corresponding ϕ_A vs z profile (Fig. 2). Since the compo-

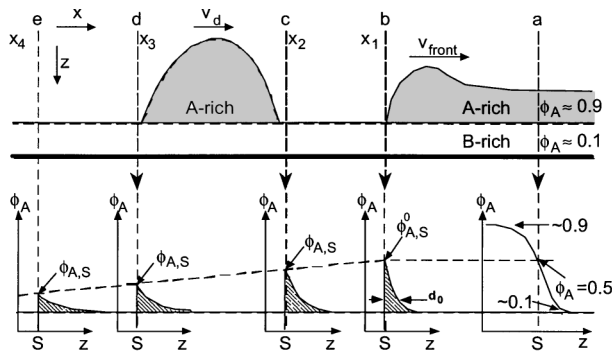


FIG. 2. Top half: schematic illustration of the dewetting of the *B*-rich substrate by the *A*-rich upper film. Composition-depth (z) profiles $\phi_A(z)$ of the *A*-rich phase taken through cuts *a*–*e* are indicated in the lower half. The decay in the surface composition $\phi_{A,S}$ of the *A*-rich phase at the surface S of the liquid substrate occurs progressively with increasing time due to diffusion of *A* into the substrate after the front has passed. The broken line in the lower half shows the decay of $\phi_{A,S}$ along the substrate surface; this decay is the origin of the surface tension gradient driving the droplets.

sition in the bulk of the *B*-rich substrate film is very different from this, with $\phi_{A,\text{bulk}} \approx 0.1$, the surface composition at x_1 ($\phi_A \approx 0.5$) is out of equilibrium and begins to relax by diffusion towards $\phi_{A,\text{bulk}}$. Regions of the substrate film that were exposed by dewetting the top layer at positions x_2, x_3 , etc., at earlier times t_2, t_3 , etc., will by then have relaxed progressively further toward $\phi_{A,\text{bulk}}$, as indicated in the corresponding ϕ_A vs z profiles (cuts *c, d*, and *e* going from right to left in Fig. 2). This implies that there will be a gradient ($\partial\phi_A/\partial x$) in the volume fraction $\phi_A = \phi_{A,S}$ along the substrate surface, with $\phi_A \approx 0.5$ just near the dewetting front, and progressively lower at positions that were dewetted earlier, as illustrated in Fig. 2 by the locus of $\phi_A(x)$ (broken line, lower half of Fig. 2). This gradient makes it favorable for the *A*-enriched droplets to move in the direction of the receding front (*A*-richer surface composition), which is, indeed, the direction of motion observed.

We may use this model to derive the motion of the droplets. The viscous dissipation as the droplet rolls across the substrate is balanced by the free energy change in moving across the surface energy gradient [10]. Assume for simplicity that the droplet has the shape of a rectangloid of height h_d and sides X_0 (parallel to the direction x of motion) and L ; this model is slightly artificial but contains the essential features. Then, in moving a distance δx (in a time δt), the work w done on the droplet is given by $w = F_d \delta x$, where F_d is the net force on the droplet given by $F_d = |L[\gamma(x) - \gamma(x + X_0)]|$; the term in square brackets is the difference $\Delta\gamma = X_0(\partial\gamma/\partial x)$ in substrate surface tension γ across the footprint X_0 of the droplet. Gathering terms gives $F_d = \mathcal{A}(\partial\gamma/\partial x)$ where $\mathcal{A} = LX_0$ is the droplet area. Since inertia is negligible as the droplet rolls, we expect the driving shear stress (whose origin is in the surface-tension gradient), $F_d/\mathcal{A} = (\partial\gamma/\partial x)$ to equal the viscous stress, $\sigma = (2v_d/h_d)\eta$, giving $v_d = (h_d/2\eta)(\partial\gamma/\partial x)$, which has the form of the Marangoni velocity for a droplet in a surface tension gradient [7,11]. Taking the droplet to be a spherical cap of height h_d gives a slightly different prefactor (which we ignore at this level of sophistication). We write therefore

$$v_d \approx (h_d/2\eta)(\partial\gamma/\partial x) = (\alpha D_d/4\eta)(\partial\gamma/\partial x), \quad (1a)$$

where the cap height h_d is related to its diameter D_d as $h_d = \alpha(D_d/2)$, with α a constant depending on the contact angle [12]. The initial value of the droplet velocity $v_{d,0}$, just after it has calved from the dewetting rim, is given by

$$v_{d,0} = (\alpha D_d/4\eta)(\partial\gamma/\partial x)_0, \quad (1b)$$

where we expect the initial value $(\partial\gamma/\partial x)_0$ to be constant for a given liquid-liquid system. The motion of a liquid rim on a liquid substrate has been considered in detail [3]: Under conditions where the rim height h_d is much greater

than the substrate film thickness, and where the viscosity of the substrate liquid $\eta_B > \eta_A/\theta$, where η_A is the viscosity of the rim and θ is the dihedral angle at the rim/substrate interface, the liquid substrate behaves effectively as a solid [3,11], i.e., stick boundary conditions and little dissipation in the substrate film. These assumptions underpin Eq. (1), and are in practice close to the conditions in our study. Thus, the droplet heights, of order $10 \mu\text{m}$, are much larger than the substrate film thickness (of order 200 nm). The viscosity mismatch is also approximately valid for both types of bilayers studied: for the OEP/dOS combination, the top dewetting layer and droplets are the less viscous dOS-rich phase, while for the OEP/hOS combination it is the less viscous OEP-rich phase that is on top. We note that $(1/\theta) \leq \text{ca. } 2\text{--}3$ [13], while (Table I) $\eta_{\text{OEP}} \approx 3.3\eta_{\text{dOS}}$ and $\eta_{\text{hOS}} \approx 2\eta_{\text{OEP}}$, comparable to the crossover value $(1/\theta)$ (though the presence of wakes following the droplets suggests that there is some dissipation in the substrate film).

Thus, from Eq. (1b) we expect the initial velocities of the droplets $v_{d,0}$ to increase linearly with cap diameter D_d . In Fig. 3 we plot $v_{d,0}$ vs D_d for the two liquid pairs in our study, over a range of droplet sizes [deduced from data such as in Fig. 1(c)]: Within the scatter, the linear relation of Eq. (1b) is indeed obeyed.

A complete picture of the droplet motion requires the evaluation of $(\partial\gamma/\partial x)$. The surface tension, $\gamma(x, t)$, will be a function of the surface composition $\phi_{A,S}(x, t)$, which in turn will depend on the time t elapsed since the front passed the point x (since that is the time over which relaxation by diffusion towards $\phi_{A,\text{bulk}}$ occurs). Take the value of the surface tension difference between the A (rich) phase (which is the phase of which the droplet is composed) and the B (rich) phase to be $\Delta\gamma_0$, and assume

$$(\partial\gamma/\partial x) = \Delta\gamma_0 \phi_{A,S}^0 d_0 [(1/\sqrt{Dt_m}) - (1/\sqrt{Dt_n})] / [v_{\text{front}}(t_n - t_m)]. \quad (2)$$

To proceed we substitute for v_{front} , whose time variation is well described by $v_{\text{front}} \equiv v_{f,0}(t/t_{f,0})^{-0.5}$, where $v_{f,0}$ and $t_{f,0}$ are characteristic values [5]. We then substitute for $(\partial\gamma/\partial x)$ from Eq. (1) (recalling $v_d = v_{d,0}$ at $t = 0$) to obtain a relation for $v_d \equiv (dx_d/dt)$, where $x_d(t)$ is the droplet displacement at time t , and finally we go to the continuous limit and integrate (recalling $x_d = 0$ at $t = 0$) to obtain [14]

$$x_d(t) = C \ln[t/t_0 + 1], \quad (3)$$

where $C = (\alpha D_d \Delta\gamma_0 \phi_{A,S}^0 d_0) / (8\eta v_{f,0} \sqrt{Dt_{f,0}})$ and $t_0 = C/v_{d,0}$. This is the relation we have been seeking: all the parameters predicting $x_d(t)$ in Eq. (3) are in principle determinable from experiment. We emphasize that since the ratio $D_d/v_{d,0}$ is constant for a given set of conditions (liquid/liquid pair and temperature), a single value of $C/D_d = (\alpha \Delta\gamma_0 \phi_{A,S}^0 d_0) / (8\eta v_{f,0} \sqrt{Dt_{f,0}})$ and of $t_0 = (C/v_{d,0})$ should in principle fully determine the entire

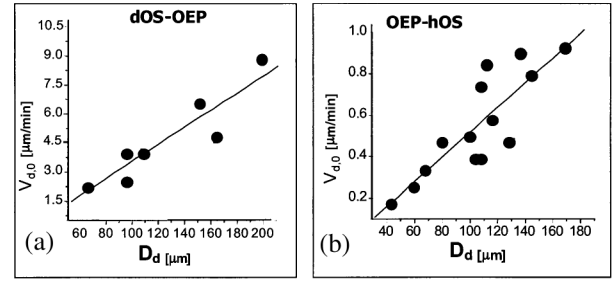


FIG. 3. Variation of initial droplet velocities $v_{d,0}$ as a function of droplet cap diameters D_d . $v_{d,0}$ is evaluated from the initial slope of the $x_d(t)$ plots corresponding to the different droplets [as in Fig. 1(c)]. (a) For the dOS-OEP couple (dOS-rich droplets on OEP-rich substrate), (b) for the OEP-hOS couple (OEP-rich droplets on hOS-rich substrate).

that the surface-tension difference $\Delta\gamma$ between the A -rich droplet and the substrate varies linearly with the volume fraction $\phi_{A,S}$ at the substrate surface, i.e., $\Delta\gamma = \Delta\gamma_0[1 - \phi_{A,S}]$. $\phi_{A,S}$ decreases from its initial value $\phi_{A,S}^0$ (cut b in Fig. 2) as the A excess at the substrate surface diffuses into the substrate film (Fig. 2). If the initial width of the A -enriched surface phase at S [just after the droplet has calved (cut b , Fig. 2)] is d_0 , it will broaden by diffusion to a value $d(t) \approx \sqrt{Dt}$, where D is the appropriate diffusion coefficient; from conservation of A we expect $\phi_{A,S}(t) \approx \phi_{A,S}^0(d_0/\sqrt{Dt})$. The difference $\delta\Delta\gamma$ in $\Delta\gamma$ between adjacent times t_m and t_n is therefore $\delta\Delta\gamma \approx \Delta\gamma_0 \phi_{A,S}^0 d_0 [(1/\sqrt{Dt_m}) - (1/\sqrt{Dt_n})]$. The corresponding lateral distance δx along the substrate surface between the two positions corresponding to these times is just $v_{\text{front}}(t_n - t_m)$, where v_{front} is the velocity of the receding dewetting front. Finally, putting $(\partial\gamma/\partial x) = (\delta\Delta\gamma/\delta x)$ and gathering all the terms above, we find that this gradient is given by

range of behavior for droplet motion in any given system. We carry out such a fit to the data for all five droplet diameters in Fig. 1(c), as shown by the solid curves. The values used, $C/D_d = 0.44$ and $t_0 = 62.5 \text{ min}$, are well within the range of the predicted absolute magnitudes $C/D_d = 0.15\text{--}0.46$ and $t_0 = 32\text{--}97 \text{ min}$ for the OEP-hOS couple of Fig. 1(c) (where the range in the predicted values arises from the range of experimental uncertainty in the defining parameters, particularly in the mutual diffusion coefficient [15,16]). Bearing in mind that there are no adjustable parameters, the predicted magnitude and, especially, the predicted time variation of $x_d(t)$ fit all the data very closely. Similarly good fits of predicted to observed droplet motion $x_d(t)$ are obtained for the liquid pair dOS/OEP (not shown). We note also that the actual magnitude of $(\partial\gamma/\partial x)_0$ required to move the droplets at the observed velocity is tiny: At ca. $3 \times 10^{-3} \text{ (N/m)/m}$ [for the OEP/hOS pair, Fig. 1(c)] it is

some 3 orders of magnitude smaller than the gradient in surface tension [ca. 2 (N/m)/m] required for the Marangoni effect to initiate the liquid-liquid dewetting at the sample edges in the first place. This also implies that droplet asymmetry arising from contact angle variations due to changes in γ along the surface is negligible.

In summary, we have found that droplets formed in the dewetting process of partially miscible liquid films that dewet via the formation of a front continue to move for extended periods in the direction of the receding front with a velocity that decays with time. We attribute this to a surface energy gradient arising from progressive relaxation of the surface composition towards its equilibrium value following the dewetting, balanced by viscous dissipation in the rolling droplets. A model based on these ideas enables us to calculate, with no adjustable parameters, the absolute values of the spontaneous droplet displacement $x_d(t)$ and its variation with time. The predictions of the model, that $v_{d,0}$ increases linearly with the droplet size and that $x_d(t)$ varies logarithmically with time, are closely consistent with our observations.

Donations of the dOS by M. Wilhelm (MPI Polymerforschung, Mainz) and the OEP by L. J. Fetters (Cornell University) are gratefully acknowledged. We thank the German-Israel Foundation (GIF), the U.S.-Israel BSF, and the Israel Science Foundation for support of this work. We appreciate useful comments by Robin Ball, Allon Klein, Tom Witten, and Stephan Herminghaus.

*Present address: Physikalisches Institut, Universität Karlsruhe, D-76128 Karlsruhe, Germany.

†Present address: Contitech Vibration Control GmbH, Jädekamp 30, Postfach 169, D-30001 Hannover, Germany.

‡Electronic address: rachely@bgumail.bgu.ac.il

§Corresponding author.

Electronic addresses: jacob.klein@weizman.ac.il or jacob.klein@chem.ox.ac.uk

- [1] A. Vrij, *Discuss. Faraday Soc.* **42**, 23 (1967).
 [2] L. Leger and J.F. Joanny, *Rep. Prog. Phys.* **55**, 431 (1992); R.A. Segalman and P.F. Green, *Macromolecules* **32**, 801 (1999).
 [3] F. Brochard-Wyart, P. Martin, and C. Redon, *Langmuir* **9**, 3682 (1993).

- [4] R. Yerushalmi-Rozen, T. Kerle, and J. Klein, *Science* **285**, 1254 (1999).
 [5] T. Kerle, J. Klein, and R. Yerushalmi-Rozen, *Langmuir* **18**, 10146 (2002).
 [6] M.K. Chaudhury and G.M. Whitesides, *Science* **256**, 1539 (1992).
 [7] J.B. Brzoska, F. Brochard-Wyart, and F. Rondelez, *Langmuir* **9**, 2220 (1993).
 [8] F.D. Dos Santos and T. Ondaçuhu, *Phys. Rev. Lett.* **75**, 2972 (1995).
 [9] A. Fery, S. Herminghaus, and M. Ibn-Elhaj, *Mol. Cryst. Liq. Cryst.* **330**, 267 (1999).
 [10] See footnote 25 of Ref. [5].
 [11] J.F. Joanny, *Phys. Chem. Hydrodyn.* **9**, 183 (1987).
 [12] For a spherical cap of height $h_d = \alpha D_d/2$, subtending a contact angle θ_p at the planar substrate, $(2\alpha/[\alpha^2 + 1]) = \sin\theta_p$; for small α , $\alpha \approx (\sin\theta_p)/2$. A plot of h_d vs D_d (obtained using optical phase interference microscopy) yielded $\alpha = 0.127$ for droplets of dOS on OEP, corresponding to $\theta_p \approx 14.5^\circ$ (≈ 0.25 rad).
 [13] For the symmetric case on a thick liquid substrate we expect $\theta = 2\theta_p \approx 0.5$ rad [12], although, because the liquid substrate is much thinner than h_d , θ is likely to be between θ_p and $2\theta_p$.
 [14] Setting $t_n = t_m + \delta t$ and $v_{\text{front}} = v_{f,0}(t_{f,0}/t)^{1/2}$ in Eq. (2) gives $(\partial\gamma/\partial x) \approx \Delta\gamma_0\phi_{A,S}^0 d_0/[8v_{f,0}(Dt_{f,0})^{1/2}(t+t_0)]$, where t_0 ensures that $(\partial\gamma/\partial x)_0$, $v_{d,0}$ remain finite at $t = 0$. Substituting in Eq. (1a) and integrating yields Eq. (3).
 [15] For the OEP/hOS couple [Fig. 1(c)] we have $\Delta\gamma_0 \approx 2 \times 10^{-3}$ N/m [4,5]; $\phi_{A,S}^0 \approx 0.5$ (Fig. 2); $d_0 \approx 10$ nm [4,5]; range of $D = (4 \times 10^{-17}) - (4 \times 10^{-16})$ m²/s [16]; $v_{f,0} = 20 \pm 5$ $\mu\text{m}/\text{min}$, $t_{f,0} = 30 \pm 7$ min [5]; $\alpha = 0.13$ [12]; $\eta = 5$ Pa s (Table I).
 [16] The mutual diffusion coefficient D of the surface OEP-rich phase into the hOS-rich substrate is difficult to evaluate with precision. It will be reduced relative to the self-diffusion coefficient D_s due to unfavorable OEP/hOS segmental interactions, and will also vary as $\phi_{A,S}$ decreases. D_s for these very short chains, where hydrodynamic screening is not expected, is estimated as $D_s = k_B T / (6\pi\eta N a)$, where a is the size of a backbone unit (ca. 0.2–0.3 nm) and N is the number of such units on the oligomers (ca. 10 and 140, respectively, for the hOS and OEP). The estimated value of D in [15] represents the mean of the two self-diffusion values (OEP and hOS), reduced by 1–2 orders of magnitude to allow for the unfavorable interactions between hOS and OEP.